Molecular Phylogenetics and Evolution 57 (2010) 1149–1161

Contents lists available at ScienceDirect

Molecular Phylogenetics and Evolution

journal homepage: www.elsevier.com/locate/ympev

Diversification in subtropical mountains: Phylogeography, Pleistocene demographic expansion, and evolution of polyphenic mandibles in Taiwanese stag beetle, *Lucanus formosanus*

Jen-Pan Huang [1], Chung-Ping Lin *

Department of Life Science & Center for Tropical Ecology and Biodiversity, Tunghai University, Taichung 40704, Taiwan

ARTICLE INFO

Article history:
Received 29 March 2010
Revised 24 August 2010
Accepted 17 October 2010
Available online 28 October 2010

Keywords:
Pleistocene
Demographic expansion
Morphological cline
Exaggerated weapon
Central mountain range
Stag beetles
Lucanidae

ABSTRACT

Pleistocene glacial oscillations have had profound impacts on the historical population dynamics of extant species. However, the genetic consequences of past climatic changes depend largely on the latitude and topography of the regions in question. This study investigates the effect of Pleistocene glacial periods and the Central Mountain Range on the phylogeography, historical demography, and phenotypic differentiation of a montane forest-dwelling stag beetle, *Lucanus formosanus* (Coleoptera: Lucanidae), which exhibits extensive mandible variations across mountain ranges in subtropical Taiwan. Analyses of mitochondrial (*cox1*) and nuclear (*wg*) loci reveal that *L. formosanus* originated nearly 1.6 million years ago (Mya) in the early Pleistocene period and consisted of geographically overlapping Alishan and Widespread clades. A drastic population expansion starting approximately 0.2 Mya in the Widespread clade likely resulted from altitudinal range shift of the temperate forests, which was closely tied to the arrival of the Riss glacial period in the late Middle Pleistocene. A ring-like pattern of historical gene flow among neighboring populations in the vicinity of the Central Mountain Range indicates that the mountains constitute a strong vicariant barrier to the east–west gene flow of *L. formosanus* populations. A geographic cline of decreasing mandible size from central to north and south, and onto southeast of Taiwan is inconsistent with the low overall phylogeographic structures. The degree of mandible variation does not correlate with the expected pattern of neutral evolution, indicating that the evolutionary diversification of this morphological weapon is most likely subject to sexual or natural selection. We hypothesize that the adaptive evolution of mandibles in *L. formosanus* is shaped largely by the habitat heterogeneity.

1. Introduction

The climatic oscillations of the Pleistocene have had profound impacts on the population dynamics and genetic constitution of extant species (Avise, 2000, 2004; Hewitt, 1996, 2000). The effects of glacial expansions and contractions on genetic heritage depend largely on latitude and topography in various parts of the globe (Hewitt, 2000, 2004). Species in lower latitudes of the temperate zone often show relatively high genetic diversity because of postglacial admixture of lineages from separate refugia. On the other hand, species in higher latitudes usually show relative low genetic variation due to rapid postglacial expansion or recolonization (Brunsfeld et al., 2001; Hewitt, 2004; Weiss and Ferrand, 2006). A few comparative studies in the tropics have shown greater genetic diversity and limited demographic expansions in tropical species compared to their temperate counterparts as a consequence of past climatic oscillations (e.g., Lessa et al., 2003; Wüster et al., 2005). Despite great advances and emerging patterns in temperate species and a few tropical species, the general effects of Pleistocene ice ages on the species in the rest of world remain unknown. This is particularly true for the tropics and subtropics (Hewitt, 2000, 2004; Beheregaray, 2008).

Taiwan is unique among all subtropical regions because it is the only sizeable island located immediately north or south of the tropical zone between the 23rd parallels. Geologically speaking, Taiwan is a relatively young island that was created by the collision of the Philippine Sea plate and Eurasian plate beginning around 9 Mya (Sibuet and Hsu, 2004). The island of Taiwan rose above sea level about 5 Mya in the early Pliocene, with tectonic uplift forces continuously building its mountain ranges (Huang et al., 2006). The Central Mountain Range (CMR) of Taiwan reached its present altitude approximately 1 Mya, and now contains more than 200 peaks exceeding 3000 m (Liu et al., 2000; Sibuet and Hsu, 2004; Huang et al., 2006). This massive CMR dominates the current landscape

* Corresponding author. Address: No. 181, Sec. 3, Taichungkang Rd., Department of Life Science, Tunghai University, Taichung 40704, Taiwan. Fax: +886 423590296.
E-mail addresses: huangjp@umich.edu (J.-P. Huang), treehops@thu.edu.tw (C.-P. Lin).
[1] Present address: Museum of Zoology, University of Michigan, 1109 Geddes Avenue, Ann Arbor, MI 48109, USA.

1055-7903/$ - see front matter © 2010 Elsevier Inc. All rights reserved.
doi:10.1016/j.ympev.2010.10.012

of Taiwan, which stretches only about 400 km long and 150 km wide. The CMR transects the island from north to south and leaves only a small portion of flat plains along the southwest coast. The topographic complexity and high altitude of the CMR in subtropical Taiwan is significant because it provides a great variety of altitudinal and climatic habitats, and serves as a physical barrier to species movement and gene flow among populations. The high endemism of terrestrial fauna and flora located on mountain tops and along altitudinal gradients implies that the CMR play a central role in the divergence and speciation of Taiwan's species (Yu, 1994; Hsieh, 2002).

Though the expanding ice sheets of recent ice ages never reached Taiwan, the remarkable climatic changes of the Pleistocene have shaped the population dynamics of the island's species (Hwang et al., 2003; Cheng et al., 2005; Chen et al., 2006; Lin et al., 2008). During the cool climate of the Pleistocene glacial periods, subtropical montane species in the mid- to higher altitudes of Taiwan descended and expanded to lower elevations following the altitudinal range shifts of temperate forests (Tsukada, 1966, 1967; Liew and Chung, 2001). As the climate became warmer during interglacial periods, a reverse sequence of events occurred, with montane species in the lowlands retreating to higher altitudes following the range contractions of temperate forests. As a result, the extant montane species in higher altitudes of Taiwan experienced repeated demographic and spatial expansions in recent Pleistocene glacial periods, and survived subsequent climatic oscillations in the same region. This study examines the phylogeography and population genetic structure of a polyphenic stag beetle, *Lucanus formosanus* Planet, 1899 (family Lucanidae), a montane forest-dwelling insect whose distribution covers most of the mountain ranges in Taiwan, to test the predictions derived from the Pleistocene expansion hypothesis. This study also investigates the effects of CMR on the genetic structure of *L. formosanus*.

Lucanus formosanus is one of the 23 lucanid species endemic to subtropical Taiwan, and inhabits broadleaf deciduous forests at elevations of 500 to 1600 m (Chang, 2006). Like most stag beetles, *L. formosanus* males have greatly enlarged, curved mandibles. They use these mandible weapons in combat with male opponents over access to feeding sites, such as tree sap locations frequently visited by females (Fig. 1A–D) (Tatsuta et al., 2001, 2004; Harvey and Gange, 2006; Kodric-Brown et al., 2006). Although the size and shape of the mandible and clypeus are often diagnostic for *L. formosanus*, populations in different mountains exhibit three major morphs (Wang, 1987, 1990, 1994) (Fig. 1B–D): (1) the Northern morph, with a median size mandible and a Y-shaped clypeus, (2) the Central morph, exhibiting the largest mandible and a highly developed Y-shaped clypeus, and (3) the Southern morph, having a shorter mandible and poorly developed clypeus. The presence of extensive geographical variations in mandible forms raises the questions of whether or not *L. formosanus* from different mountain ranges display discrete phenotypic or genetic subdivisions. A phylogeographically structured *L. formosanus* would be consistent with the hypothesis that the CMR has been a strong vicariant barrier affecting lineage diversification in Taiwan.

This study first quantifies the level of morphological differentiation in *L. formosanus*, and determines if populations from different mountain ranges exhibit distinct phenotypic subdivisions or if mandible variation is continuous and clinal in nature. Secondly, this study infers the phylogeography, population genetic structure, and historical demography of *L. formosanus* using DNA sequences from both mitochondrial and nuclear loci. We predict that the montane forest-dwelling *L. formosanus* that experienced Pleistocene glacial expansion events over its present subtropical mountain ranges would exhibit several characteristics: (1) a shallow phylogeny and little population subdivision, (2) a unimodal mismatch distribution of pairwise nucleotide differences, indicating a sudden demographic expansion, (3) a rapid increase in estimated effective population sizes over time, with the onset of historical population growth temporally coupled with major glacial periods, (4) low historical gene flow between the eastern and western CMR populations compared to the relatively higher gene exchange among populations on each side of the CMR. Finally, this study discusses the evolutionary diversification of polyphenic mandibles in *L. formosanus* using reconstructed phylogeography and demographic history.

2. Material and methods

2.1. L. formosanus and population sampling

L. formosanus adults emerge mostly between June and September to feed on saps of the Griffith ash, *Fraxinus griffithii* (Oleaceae) and Ring-cupped oak, *Cyclobalanopsis glauca* (Fagaceae). They usually fly up to the canopy of forests during the daytime hours and are attracted to artificial lights in the evening (Chang, 2006). A total of 52 *L. formosanus* from 25 localities around Taiwan were collected and assigned to seven mountain ranges (Fig. 1F; Supplementary data), including Shueshan (SS, which is located within the range north of the Tachia river and west of the Lanyang river), West Central Mountain Range (WCMR, including mountains west of the Central Mountain Range, CMR and separated from Yushan and Alishan mountain ranges by Choushui and Laonung rivers), South Central Mountain Range (SCMR, including LC population located near the southern tip of CMR and nearby populations, i.e., LC and LY), East Central Mountain Range (ECMR, including two individuals from JS), Coastal Range (CR, an isolated mountain chain located at eastern Taiwan), Yushan (YS, the highest mountain range surrounded by Choushui, Chishan, and Laonung rivers, i.e. JL), and Alishan (ALS, which constitutes a mountain range south of the Choushui river and west of the Chishan river). These insect specimens were kept in 95% EtOH and a −20 freezer. The vouchers were stored in −80 °C freezers located at the insect collection of Tunghai University. The specimen of the outgroup taxon, *L. hermani* DeLisle, 1973 of China, was obtained from a commercial insect supplier (http://www.insect-sale.com). *L. hermani* is among the closest related *Lucanus* species of *L. formosanus*. A recent molecular phylogeny of endemic Taiwanese *Lucanus* species suggested their sister relationship (Lin et al., 2009).

2.2. DNA extraction and sequencing

Genomic DNAs of *L. formosanus* and outgroup species were extracted from the beetle's thoracic muscle using MasterPure™ DNA Purification Kit (EPICENTRE® Biotechnologies, Madison, WI). A fragment of approximately 1300 bps of mitochondrial *cox1* (cytochrome oxidase I subunit) gene was amplified using a *Lucanus*-specific primer set (*Lucanus*-COI-J-1751, 5′-GAGCTCCTGATATAG CTTTTCC-3′ and *Lucanus*-TL2-N-3014, 5′-CCAATGCACTAATCTGC CATATTA-3′) (Lin et al., 2009). In addition, a nuclear *wg* (*wingless*) gene of about 500 bps was amplified for most specimens using a primer set of *wg*1a and *wg*2a (Brower and DeSalle, 1998). *Wg* fragments of remaining specimens were amplified using *wg*1a and a newly developed *Lucanus*-specific primer, *Lucanus*-*wg*2a (5′-TTGCACCTTTCGACGATGGCGATCTC-3′) (Lin et al., 2009). The PCR profile was as following: (1) an initial denaturation at 94 °C for one minute, (2) followed by 35 cycles of denaturation at 94 °C for one minutes, annealing at 55 °C for one minute, and an extension at 72 °C for one minute, and (3) a final extension step at 72 °C for ten minutes. The annealing temperature for *wg* was 55 to 60 °C. The 50 μl PCR reactions contained 1 μl of genomic DNA, 21.75 μl of

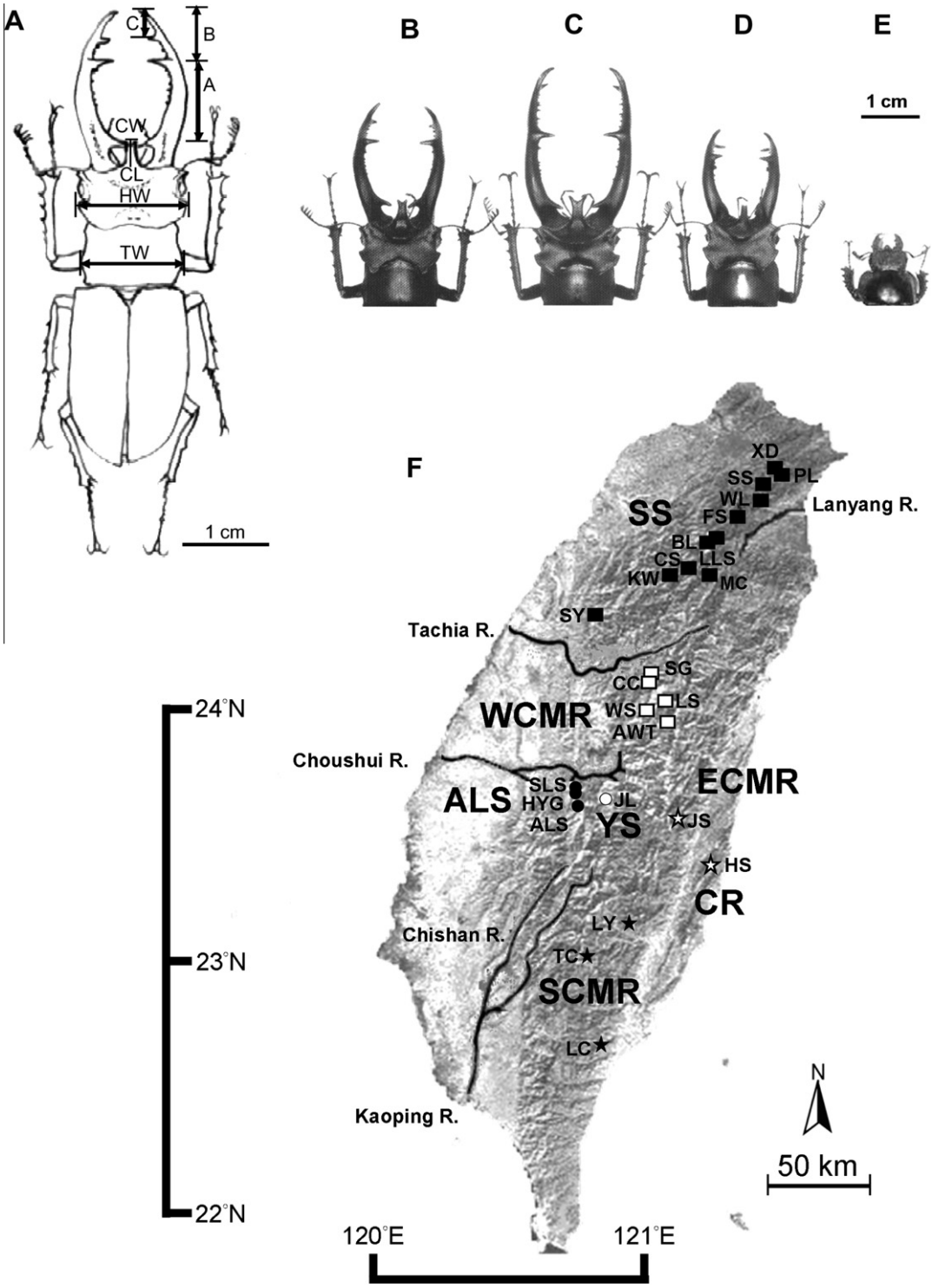

Fig. 1. (A) Measurements of seven body parts used for morphological analyses of *L. formosanus*. A, B, and C, lengths of three sections of mandible; CL, clypeal length; CW, clypeal width; HD, head width; TW, thorax width. (B) Northern, (C) Central, and (D) Southern morphs of male *L. formosanus*. (E) A female of *L. formosanus*. (F) Sampling sites and their corresponding mountain ranges. SS, Shueshan Mountain range; WCMR, Western Central Mountain Range; ALS, Alishan Mountain Range; YS, Yushan Mountain Range; SCMR, Southeastern Central Mountain Range; CR, Coastal Range. Names of abbreviation of sampling sites are listed in Supplementary data.

ddH_2O, 10 μl of 1 mM dNTP, 10 μl of 5 × GoTaq colorless buffer, 5 μl of 25 mM $MgCl_2$, and 0.25 μl of 5u/μl GoTaq (Promega, Madison, WI, USA). The PCR products of *wg* amplifications were pooled from five smaller 10 μl reactions. The successfully amplified PCR products were gel-purified and extracted using Gel/PCR DNA Fragments Extraction Kit (Geneaid, Taipei, Taiwan), and then cloned into competent cells (DH-5α) (Protech, Taipei, Taiwan) using T&A cloning kit (RBC, Taipei, Taiwan). DNA sequencing was performed on an ABI PRISM™ 377 automatic sequencer (Perkin Elmer, USA) by the Mission Biotech, Taiwan.

2.3. Neutrality of sequence evolution

DNA sequences were aligned using Clustal W method in MegAlign (DNASTAR, Madison, USA). The aligned *cox1* and *wg* sequences were translated into amino acid sequences in MacClade

(v. 4.06, Maddison and Maddison, 2000) using the mitochondrial genetic code of the *Drosophila* and a universal genetic code of nuclear genes respectively to confirm codon assignment and possible stop codons caused by ambiguous sequencing. We used McDonald Kreitman Test (MKT) implemented in DnaSP (v. 4.0, Rozas et al., 2003) to detect the signature of natural selection at *cox1* and *wg* by comparing proportions of synonymous and nonsynonymous substitution within vs. between populations. The significance of deviations on the ratio of replacement to synonymous substitutions was determined by two-tailed Fisher's exact tests. Neutral evolution of the two genes was further assessed using a codeml module of PAML (v. 4, Yang, 2007). For *cox1*, all sites were included in the analysis except for one stop codon (TAA) and tRNA-Leu region. The nonsynonymous versus synonymous substitution ratio (ω: d_N/d_S) was first calculated under model 0 (no site rate heterogeneity) with likelihood tree topologies obtained from the phylogenetic analyses. We then calculated the likelihood values of six site-specific models, and the Likelihood Ratio Tests (LRT) were used to detect the significance between nested models using chi-square statistics. These nested models were: (1) model 0 versus model 3, which was used to test for site rate heterogeneity of amino acid sequences, (2) model 1 versus model 2, testing for neutrality versus selection, and (3) model 7 versus model 8, which was further used to test for positive selection.

2.4. Phylogenetic analyses

We conducted maximum parsimony (MP) analyses using the parsimony ratchet procedure (Nixon, 1999) implemented in PAUPRat (Sikes and Lewis, 2001) and PAUP* (v. 4.0b10, Swofford, 1998) to search for the most parsimonious trees. Parsimony branch supports were calculated using non-parametric bootstrapping with 1000 iterations, each with 10 stepwise random sequence additions and the tree-bisection and reconnection (TBR) branch swapping. For maximum likelihood (ML) and Bayesian analyses, the best-fitted nucleotide substitution models for each gene were determined separately in MODELTEST (v. 3.7, Posada and Crandall, 1998) using Bayesian Information Criterion (BIC). Parameter values derived from the best-fitted model were subsequently used in likelihood analyses. We calculated likelihood scores of all obtained MP tree topologies under the best-fitted substitution models, and then used the tree topology with the highest likelihood score as a starting tree in heuristic ML tree searches. The heuristic ML search procedures were repeated four times until the likelihood scores were in a stasis. ML branch supports were calculated with 100 bootstrap replications with neighbor-joining (NJ) starting trees and TBR branch swapping. Bayesian posterior probabilities (BPP) of the trees were calculated using MrBayes (v. 3.1.2, Huelsenbeck and Ronquist, 2001). Two independent Bayesian analyses with random starting trees were run. In each analysis, two independent runs were performed simultaneously with each run containing four Markov Chains. MCMC searches were performed for 3×10^6 generations with Markov chains being sampled for every 100 iteration. MCMC searches were terminated after the average split frequencies of two runs falling below the value of 0.01, and the convergence diagnostic potential scale reduction factor reaching 1 indicating the convergence of separate runs (Gelman and Rubin, 1992). The initial 7500 MCMC samples were discarded as burn-in. The remaining trees (22,500) were imported into PAUP* to compute a 50% majority rule tree with the percentage of trees recovering the node representing the node's posterior probability.

2.5. Phylogeographic and population genetic analyses

Nested clade phylogeographic analysis (NCPA, Templeton et al., 1995; Templeton, 2008, 2009) was used to investigate the association between population divergence, geographic distances, and historical events. The haplotype network with 95% confidence intervals was reconstructed using TCS (v. 1.21, Clement et al., 2000). This parsimony network was nested according to the rules of Templeton et al. (1992) and used in GeoDis (v. 2.5, Posada et al., 2000) to calculate clade distance (D_c) and nested clade distance (D_n). When significant values of D_c or D_n were detected, the revised inference key (Templeton, 2004) was used to discriminate historical effects of restricted gene flow, past fragmentation, and range expansion. Haplotype diversity (h), nucleotide diversity (π), population differentiation (F_{ST}), and the effective gene flow (Nm) of populations were estimated using DnaSP. The significance of genetic differentiation among populations was assessed using Hudson's nearest neighbor statistics (S_{NN}) with 1000 permutations in DnaSP. S_{NN} will be close to 1 if populations were strongly structured, or 1/7 if populations were completely unstructured (Hudson, 2000). Analysis of Molecular Variance (AMOVA) was conducted in ARLEQUIN (v. 3.01, Excoffier et al., 2005) with 10,000 permutations to assess the degree of genetic divergence among mountain ranges (Φ_{CT}), within mountain ranges among populations (Φ_{SC}), and within populations (Φ_{ST}).

2.6. Historical demography, gene flow, and divergence times

The demographic history of *L. formosanus* was inferred based on *cox1* using the mismatch distribution with 1000 bootstrap replications in ARLEQUIN. The goodness of fit between the observed and expected distributions of demographic models, including sudden expansion and spatial expansion with constant deme was calculated using Sum of Square Deviations (SSD). The Harpending's Raggedness Index (r) was calculated to evaluate the roughness of the observed curves, in which a smaller r represents a smoother curve (Rogers and Harpending, 1992). The significance of r was calculated using a null distribution simulated from 1000 permutations in ARLEQUIN. The past population dynamics of *L. formosanus* through time was further estimated using a coalescent-based Bayesian Skyline Plot without the assumption of particular demographic models (Drummond et al., 2005). The posterior probability distribution of effective population sizes ($N_e\tau$) and Time to the Most Recent Common Ancestor (T_{mrca}) were estimated in BEAST (v. 1.4.8, Drummond and Rambaut, 2007) using the best-fitted model of nucleotide substitution and their parameter values as priors. Bayesian Skyline Plot analyses were done separately using haplotypes found only in the Widespread and Alishan lineage (Fig. 2A). Nucleotide substitution rate of *cox1* was set to the average value commonly found in arthropods (1.15% divergence/lineages/million years; Brower, 1994; Balke et al., 2009; Pons et al., 2010; Ribera et al., 2010) with a strict molecular clock. The group size of Bayesian Skyline Plot was set to 10 and four respectively for the Widespread and Alishan lineages identified in network analyses. MCMC samplings were run for 1×10^8 generations with parameters sampled for every 1×10^4 generation. The initial 10% of the run was discarded as burn-in. Each analysis was repeated multiple times to optimize the scale factors until no suggestion message appeared on the log file. The Effective Sample Size (ESS) for the posterior distribution of estimated parameter values was determined using Tracer (v. 1.4, Rambaut and Drummond, 2007).

The level of gene flow among populations was estimated as ancestral migration using Bayesian coalescent-based LAMARC (v. 2.1.3, Kuhner, 2006). We estimated the population genetic parameters of effective population size (θ) and immigration (M) with the assumption of both populations and migration are at equilibrium. The immigration parameter M was considered as Nm for *cox1* and $4Nm$ for *wg*, which were obtained by multiplying

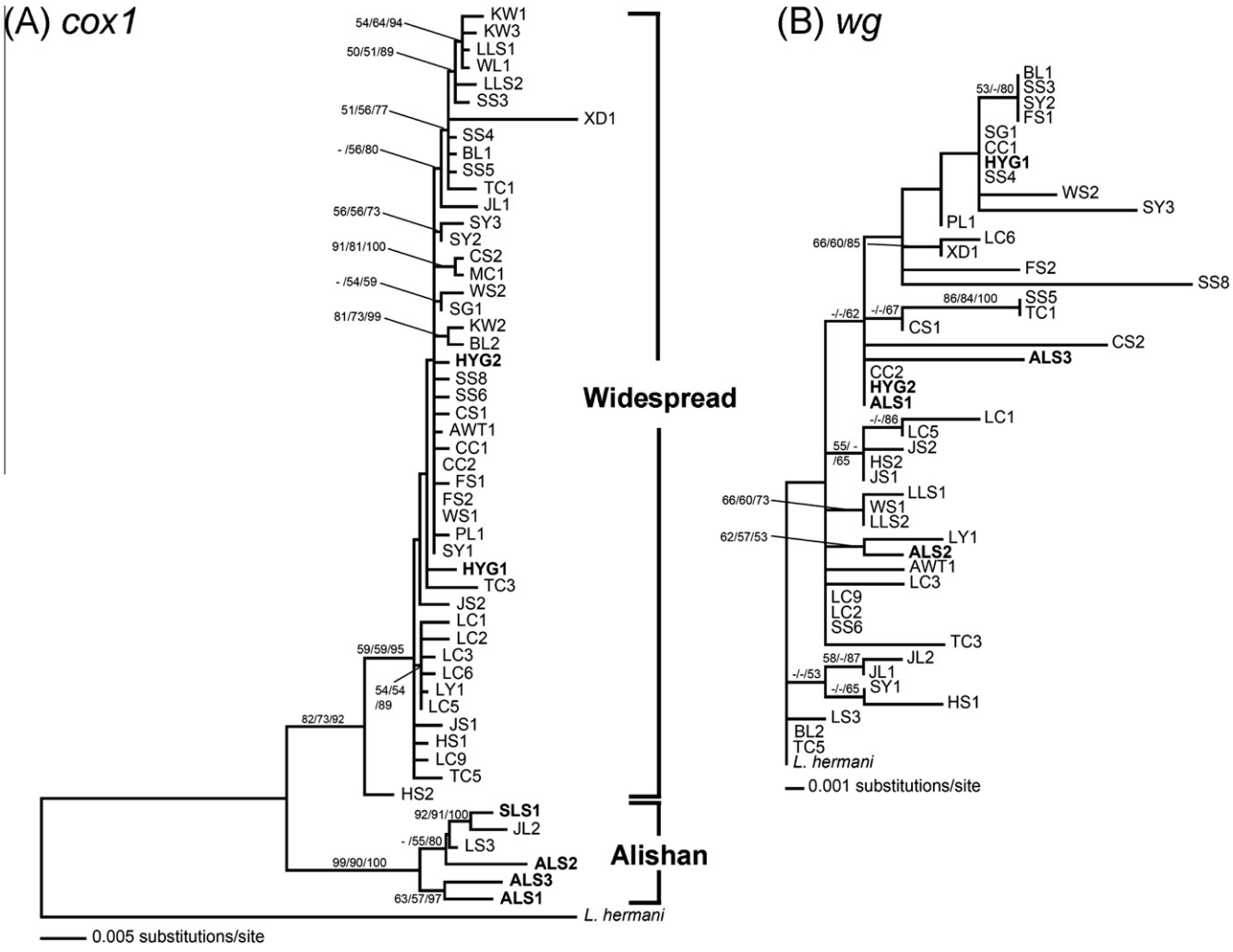

Fig. 2. The ML phylogeny of *L. formosanus* resulted from the Bayesian phylogenetic analyses based on (A) *cox1* and (B) *wg* genes. Numbers near the nodes are support values of parsimony bootstrap (left), likelihood bootstrap (center), and Bayesian posterior probability (right). Nodes without support values are those have values below 50%. Haplotypes of the Alishan region are labeled as bold.

the migration rate M and θ of recipient population ($\theta = N\mu$ for mitochondrial genes, and $\theta = 4N\mu$ for nuclear genes; $M = m/\mu$, where m is the immigration rate per generation and μ is the neutral mutation rate per site per generation). Multiple short MCMC runs were done prior to the final analysis to obtain the optimal sampling strategy for the analysis. The analysis was conducted using a initial 3×10^3 generations of sampling Markov chains with genealogies sampled for every 20 steps and the first 1000 sampled genealogies discarded. The final LAMARC analysis was then followed by a 1×10^5 final sampling chain with the first 1×10^4 samples discarded as burnin and genealogies sampled for every 50 step. The Metropolis-coupled Markov chain Monte Carlo $(MC)^3$ was used to repeat sampling chains with different starting genealogies and parameter space. The automatic chain temperature adjustment and the chain heating were turned on with four MCMC chains searching simultaneously. *Cox1* was assumed to have no recombination, whereas the recombination rate parameter, r ($r = \rho/\mu$; where ρ is the recombination rate per intersite link per generation) was estimated for *wg* ($\mu = 1$ as default setting). The population growth rate parameter, g (where $\theta_t = \theta_{\text{modern}}^{-gt}$) was calculated to exam whether *L. formosanus* underwent exponential growth in the past. The population growth or decline was significant if the 95% confidence interval of g did not include zero. The posterior probability densities and ESSs for these estimated population parameters were calculated in Tracer.

2.7. Morphological measurements and variation among populations

We obtained mandible and clypeal measurements of 50 male *L. formosanus* from field collected beetles and specimens in the museum and personal collections (Supplementary data). Measurements of the seven morphological traits were recorded with a digital caliper (±0.01 mm) (SV-03, E-BASE) (Fig. 1A). Because of substantial size variation among individuals (Chang, 2006, personal observation), we divided all six mandible and clypeal trait measurements by values of the thorax width (TW, a proxy for body size) to control allometric effect of overall size variation. The Euclidean distance matrix of the standardized trait values among specimens was calculated in PRIMER (v. 5, Clarke and Warwick, 2001). The similarity matrices of the morphological traits were then used to construct the Multi-Dimensional Scaling (MDS) plot. Analysis of Similarity (ANOSIM) was used to detect the significant level of differentiation among six mountain ranges using 1×10^6 random permutations in PRIMER. Once the significant level of population differentiation was detected, the Similarity Percentage (SIMPER) was used to quantify the relative contribution made by each morphological trait.

2.8. Tests for isolation by distance and comparison of morphological and genetic divergence

We assessed whether the morphological and molecular similarity are associated with geographic distance using the Mantel test implemented in Isolation By Distance, IBD (v. 3.15, Jensen et al., 2005). Pairwise geographic distances between populations of different mountain ranges were calculated using the GPS coordinates of the localities at the center of populations (i.e., LLS for SS, LS for WCMR, HYG for ALS, JL for YS, TC for SCMR, JS for ECMR, and HS for CR) (Supplementary data). Geographic distances for populations from either side of the CMR were estimated by summing the distances connecting the populations through SS (e.g., $DIS_{ALS\text{-}CR} = DIS_{ALS\text{-}SS} + DIS_{SS\text{-}CR}$). The mean values of mandible and clypeus traits within the same mountain range were used to calculate the pairwise Euclidean distance in PRIMER. The pairwise F_{ST} values of *cox1* between populations were calculated in IBD and used as a surrogate for genetic distances. Partial mantel tests (Legendre and Legendre, 1998) were performed to investigate if morphological distance is a function of genetic distance while controlling for the effect of geographical distance. Significance in the Mantel and partial Mantel tests were evaluated against a null distribution generated by 10,000 randomizations of distance matrices. Reduced Major Axis (RMA) regression was used to estimate the slope and intercept of the relationships, with their confidence limits evaluated by 10,000 boostrapping replicates over independent population pairs.

3. Results

3.1. Neutrality of cox1 and wg

A total of 1304 bps of *cox1* and 461 bps of *wg* sequences were obtained for *L. formosanus*, and the DNA sequence alignment contained no indels. MKTs showed no signs of any selection in either genes. No fixed nonsynonymous substitutions were found in *L. formosanus* populations. Three fixed synonymous substitutions were inferred between ALS and YS populations, but the ratio of replacement to synonymous substitutions did not significantly deviate from that of neutral expectation (Fisher's exact test, $p = 0.49$). None of the LRTs of the nested likelihood model comparisons were significant except for M0 vs. M3 in *wg* ($\chi^2 = 9.7$, $p = 0.046$), where a significantly higher likelihood value was obtained for M0. This suggests no amino acid rate heterogeneity among *wg* sites. The estimated ω ratios of both genes were much smaller than 1 (0.046 for *cox1* and 0.034 for *wg*), indicating that the models based on selection or positive selection did not fit the data significantly better than models of neutral evolution. Therefore, the possibility of neutral evolution of the nucleotide sites at *cox1* and *wg* of *L. formosanus* cannot be rejected.

3.2. Phylogenetic and phylogeographic analyses

The *cox1* and *wg* sequences in this study contained 80 and 18 parsimony informative sites, respectively. The topologies of the 200 most parsimonious trees retained from ratchet analyses of the two genes (291 steps for *cox1* and 63 steps for *wg*) were comparable to the topologies of the likelihood trees. K81uf + Γ ($\ln L = -3533.694$) and TrN + Γ ($\ln L = -1039.861$) were selected as the best-fitting models of sequence evolution for the *cox1* and *wg* genes, respectively. The reconstructed ML phylogeny of *cox1* ($\ln L = -3527.583$) revealed two geographically overlapping haplotype lineages. The first was distributed in the vicinity of the Alishan Mountain in southwestern Taiwan (Alishan clade), while the other was widely spread across the island (Widespread clade) (Fig. 2A). Two Alishan haplotypes (HYG1 & HYG2) were found in the Widespread clade, and one WCMR haplotype (LS3) was clustered within the Alishan clade. There was a distinct XD1 haplotype with a particularly long branch length in the Widespread clade. In the ML phylogeny of *wg* ($\ln L = -1024.298$), populations of *L. formosanus* show little phylogenetic substructuring with respect to their geographic distribution (Fig. 2B). Nevertheless, *wg* tree showed a close relationship among Alishan haplotypes (ALS1, ALS3 & HYG2) as compared to *cox1* tree. Because the phylogenetic relationships within the Widespread clade are little resolved and do not have strong supports, our interpretation of genealogical relationships among populations is mainly based on the results of the network analyses.

A total of 49 and 32 unique haplotypes of *cox1* and *wg*, respectively, were found in *L. formosanus* populations. Not all haplotypes were connected with 95% probability in the parsimony networks (Fig. 3). Haplotypes separated by up to 13 (*cox1*) and seven (*wg*) mutational steps were connected into a single network with greater than 95% probabilities. One *cox1* network was separated by more than 29 mutational steps (4-3 Alishan clade). In congruence with phylogenetic reconstruction, the *cox1* network was mainly partitioned into the Alishan (clade 4-3) and Widespread lineage (clade 4-1 + 4-2) (Fig. 3A). Statistically significant D_n and/or D_c were detected at the clade levels 5-1 and total network (Table 1). The total *cox1* network was inferred to be a result of allopatric fragmentation, with the Alishan lineage separated from the Widespread lineage by many mutational steps. The widespread clade 5-1 was subdivided into the Western (clade 4-1) and Southeastern lineage (clade 4-2), with their geographic associations inferred to be a pattern of past fragmentation or long distance colonization. Within the Western lineage, the Central and Northern lineage (clade 3-1) was inferred to be an interior clade, with the most ancestral (center) haplotypes belonging to WCMR (clade 1-1, CC2, WS1, SY1, SY2, SG1 and AWT1). The majority of the more derived (tip) haplotypes of clades 1-2, 2-1 and 2-2 in the Central and Northern lineage were from SS, except for a few with ECMR, YS, and ALS origins. The Central and Northern lineage was connected to two networks, the Northern (clade 3-2) lineage was found largely near SS, and the Eastern and Southern (clade 3-3) was primarily located near SCMR and CR. The Eastern and Southern lineage was further connected to the more exterior Taitung lineage (clade 3-4) located at SCMR. NCPA of *wg* haplotypes suggested a pattern of restricted gene flow with isolation by distance (Table 1). Here, statistically significant associations were detected at clade levels 2-4, 3-3, and the total cladogram (Fig. 3B). Despite the lack of a clear phylogeographic structure, the *wg* network suggested that the most ancestral haplotypes (ALS1, CC2 and HYG2 of clade 2-2; CC1, HYG1, and SG1 of clade 1-1) within the interior clade 3-2 and the exterior clade 3-1 were those located in WCMR and ALS. The more derived haplotypes within the clade 3-2 were from SS and SCMR, whereas the majority of the derived haplotypes in the more exterior clades 3-1 and 3-3 were those found at SS, SCMR, and CR.

3.3. Population genetics analyses

Haplotype diversities (h) were high, ranging from 0.952 to 1 in *cox1* and 0.9 to 1 in *wg* (Table 2). Nucleotide diversities (π) were relatively low, ranging from 0.006 to 0.038 in *cox1* and 0.002 to 0.011 in *wg*. S_{NN} was estimated to be 0.58 ($p < 0.0001$) and 0.33 ($p = 0.036$) for *cox1* and *wg*, respectively, indicating substantial genetic differentiation among populations. AMOVA revealed marginal and significant *cox1* and *wg* genetic differentiation among mountain ranges ($\Phi_{CT} = 0.008, 0.035$; $p = 0.088, 0.019$) (Table 3). However, no significant genetic differentiation was detected within populations or among populations within mountain ranges.

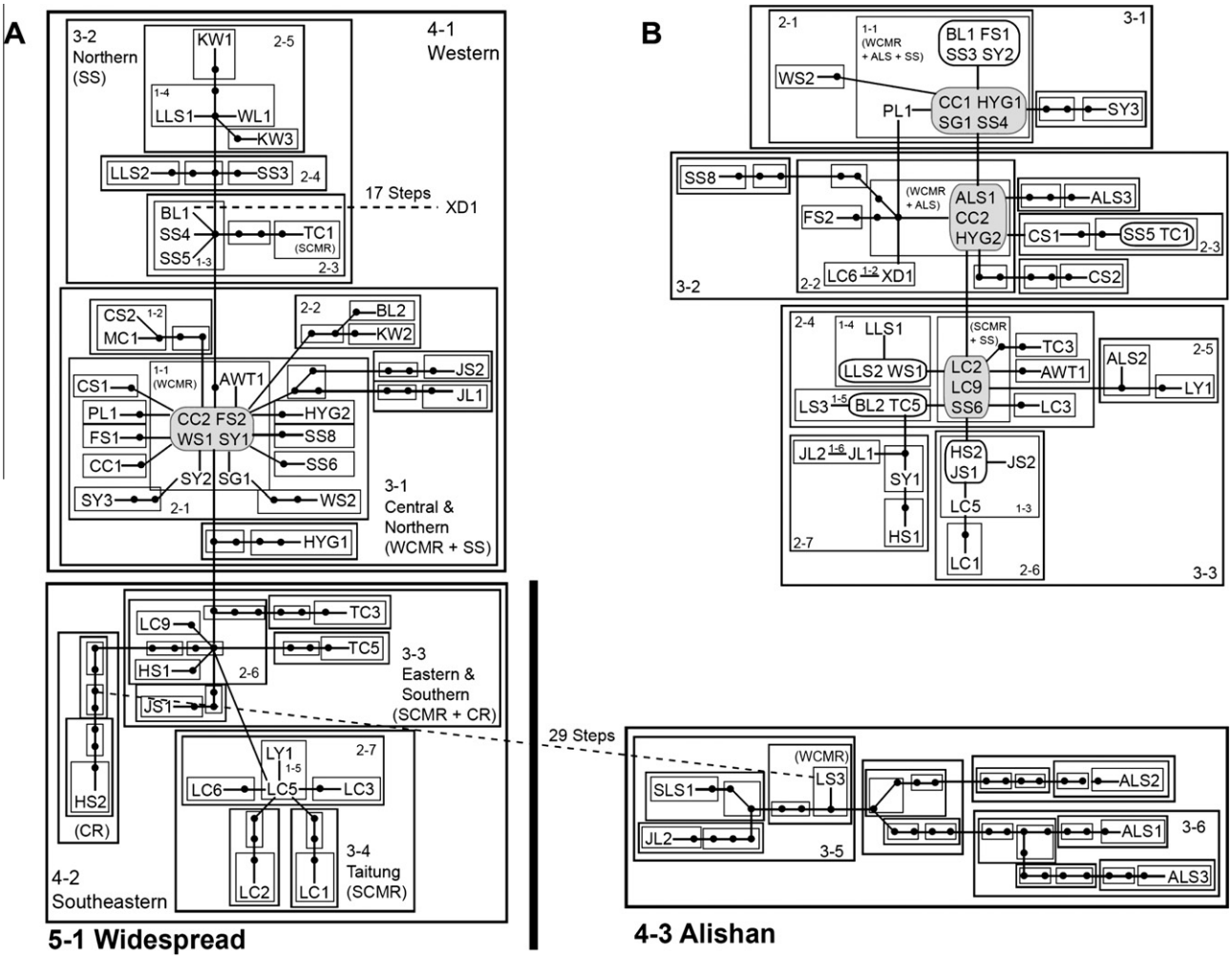

Fig. 3. Parsimony networks for (A) *cox1* and (B) *wg* haplotypes numbered by sampling sites (Supplementary data). Black dots on the network branches represent hypothetical and unobserved intermediate haplotypes. Solid branches connect haplotypes differed by one mutational step. Heavy lines encompass phylogroups where the haplotypes are connected with 95% probability. Dashes connect phylogroups and haplotypes that differ by a large number of mutational steps. The grey area contains inferred ancestral haplotypes.

Table 1
The chains of inferences for *L. formosanus* haplotype clades with significant geographic associations detected in the NCPA.

Gene	Clades	χ^2	*p* value	Chain of inference	Inference
cox1	5-1	39.95	<0.001	1-2-3-5-15-NO	Past fragmentation and/or long distance colonization
	Total	47.10	<0.001	1-2-3-4-9-NO	Allopatric fragmentation
wg	2-4	41.33	0.288	1-2-3-4-NO	Restricted gene flow with isolation by distance
	3-3	56.01	0.006	1-2-3-4-NO	Restricted gene flow with isolation by distance
	Total	45.82	0.205	1-2-3-4-NO	Restricted gene flow with isolation by distance

Table 2
Genetic diversity of *L. formosanus* populations calculated in DnaSP.

Gene		All	SS	WCMR	YS	ALS	ECMR	SCMR	CR
cox1	h	0.995	0.996	0.952	1	1	1	1	1
	π	0.012	0.006	0.010	0.038	0.025	0.007	0.006	0.010
wg	h	0.979	0.961	0.953	1	0.9	1	0.978	1
	π	0.010	0.011	0.007	0.002	0.007	0.002	0.010	0.009

Tajima's *Ds.* of the Widespread lineage of *cox1* and all populations of *wg* were negative and significantly different from 0 ($D = -2.509$ and -2.118, respectively). For the Alishan lineage of *cox1*, Tajima's *D* was negative but not significantly different from 0 ($D = -0.458$). The values of Fu's F_S for the Widespread lineage of *cox1* and all populations of *wg* were also negative and significantly different from 0 ($F_S = -24.845$ and -25.311, respectively). The Alishan lineage of *cox1* had a negative Fu's F_S value, but not significantly different from 0 ($F_S = -0.230$). Both Tajima's *D* and Fu's F_S were negative for the Widespread lineage of *cox1*, suggesting a recent population expansion.

3.4. Historical demography, divergence times, and gene flow

The mismatch distribution of the Widespread lineage of *cox1* exhibited a smooth curve with a single peak, which was not significantly different from that of a sudden expansion model (Fig. 4A). However, the distribution of the Alishan lineage had multiple peaks, indicating a stable population through time (Fig. 4B). The

Table 3
AMOVA of *L. formosanus* populations.

Gene	Source of variation	d.f.	SS	% variation	Φ	*p* value
cox1	Among mountain ranges	6	3.071	0.78	0.008	0.088
	Among populations within mountain ranges	18	8.814	−1.08	−0.011	0.058
	Within populations	27	13.5	100.29	−0.003	0.198
wg	Among mountain ranges	6	3.298	3.53	0.035	0.019
	Among populations within mountain ranges	14	6.390	−3.70	−0.038	0.559
	Within populations	25	12.333	100.17	−0.002	0.494

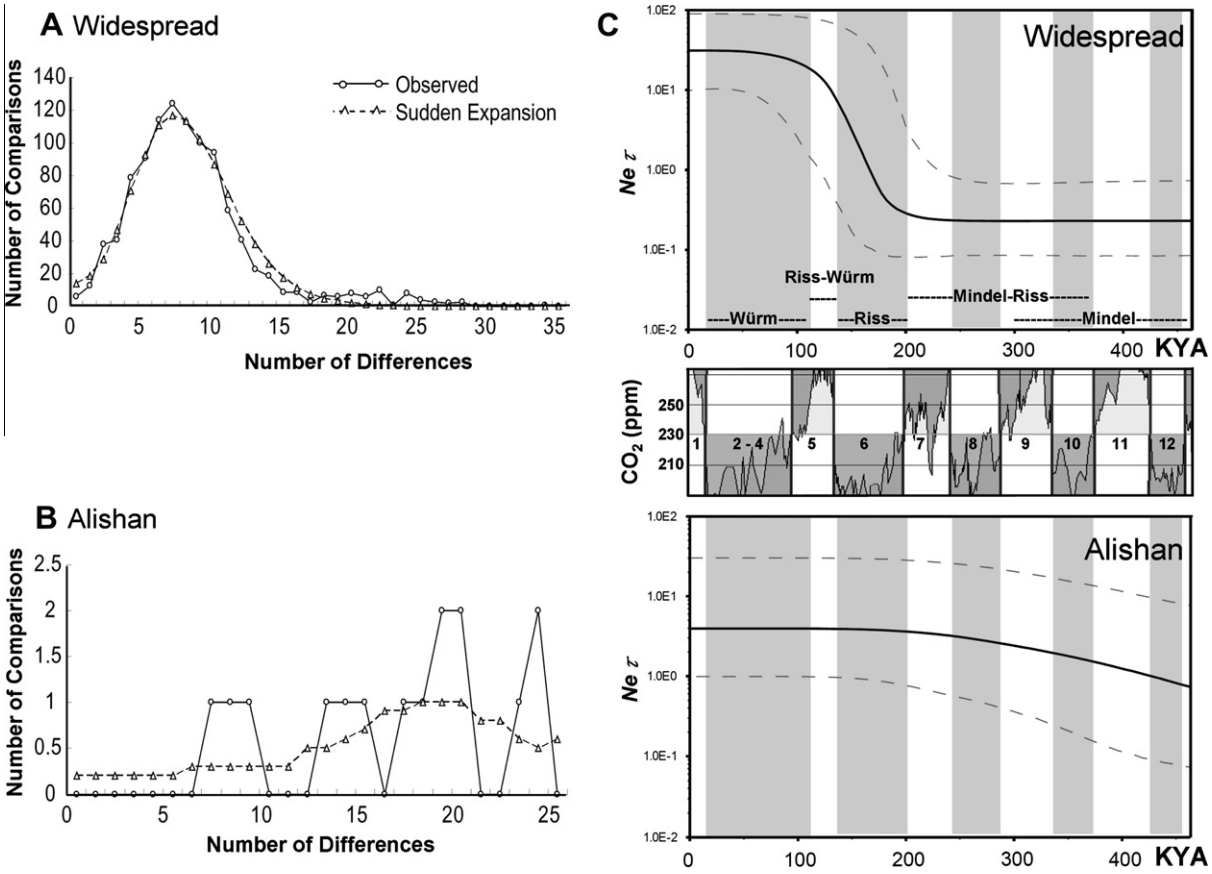

Fig. 4. Mismatch distributions of the pairwise nucleotide divergence of the (A) Widespread and (B) Alishan clade of *cox1* gene. The Widespread clade fits well with the expected model of a sudden demographic expansion (SSD = 0.00089784, $p = 0.844$; $r = 0.0050895$, $p = 0.854$; $\tau = 6.208$; $\theta_0 = 1.964$, $\theta_1 = 76.777$), whereas the Alishan clade shows a constant population through time (SSD = 0.04044936, $p = 0.668$; $r = 0.0711111$, $p = 0.918$; $\tau = 19.119$; $\theta_0 = 1.085$, $\theta_1 = 88.023$). (C) Bayesian skyline plots of the Widespread (above) and Alishan (below) clade. The center diagram shows the level of atmospheric CO_2 (Gibbard and van Kolfschoten, 2004) during the past 0.45 Mys, and numbers refers to the corresponding marine isotope stages. The shaded areas are the inferred glacial periods.

Bayesian skyline plot of the Widespread lineage with 95% HPD (Fig. 4C) demonstrated that populations had undergone a major sudden population growth starting approximately 0.2 Mya, with an estimated effective population size of 0.31 (95% HPD of $N_e\tau = 0.07–4.84$). After this period, the population grew rapidly with a more than 100-fold increase, reaching a size of 34.25 (95% HPD of $N_e\tau = 10.41–225.23$) by the end of Würm period around 0.012 Mya. On the contrary, the flat curve of the Bayesian skyline plot in Alishan lineage indicated a constant population size from 3.42 to 3.90 over the past 0.5 million years (95% HPD of $N_e\tau$ ranging from 0.33–97.72 to 0.74–100.81). T_{mrca} of *cox1* for all *L. formosanus* haplotypes was estimated at about 1.6 Mya in the early Pleistocene (Fig. 2A) (mean = 1.616 Mya, 95% CI = 1.191–2.073 Mya, ESS = 1.8×10^4). T_{mrca} for the Widespread lineage was estimated to be close to 0.7 Mya (mean = 0.735 Mya, 95% CI = 0.463–1.027 Mya, ESS = 1.3×10^4). The estimated T_{mrca} of the Alishan lineage was at about 0.5 Mya (mean = 0.478 Mya, 95% CI = 0.112–0.960 Mya, ESS = 6573).

The recombination rate (r) of nuclear *wg* was estimated to be 1.8 (95% CI = 0.494–3.124), which indicates that recombination in *wg* is about 1.8 times more likely to occur than mutation. The overall level of gene flow estimated as the past number of immigrants (Nm) in *L. formosanus* was comparable for *cox1* and *wg* when individuals were assigned into 25 populations. The estimated Nm for *cox1* increased threefold when individuals were assigned into the seven major mountain ranges. LAMARC-estimated Nm showed a pattern of non-symmetrical gene flow among populations (Fig. 5). The levels of gene flow were relatively low or nonexistent between populations located at either side of CMR compared to that on either side. Nevertheless, populations separated by CMR were genetically connected primarily through SS in northern Taiwan and SCMR in southern Taiwan. Within Western Taiwan, WCMR populations exhibited a greater amount of migration into neighboring populations than vice versa, suggesting that they functioned as a historical gene pool source. ALS, on the other hand, received large numbers of immigrants from WCMR and exchanged

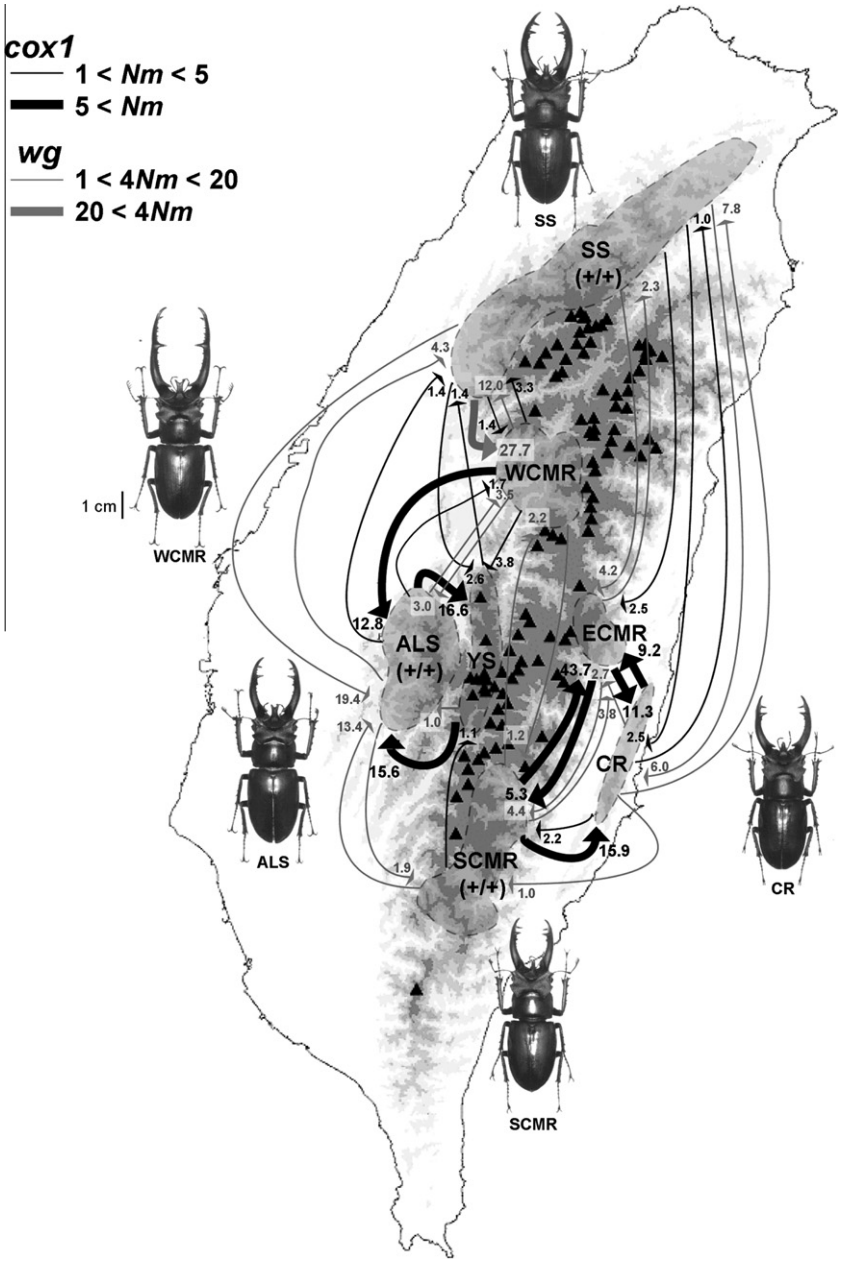

Fig. 5. Historical gene flows of *L. formosanus* populations estimated using LAMARC. Thickness of arrows represents the relative intensity of gene flow. Numbers near the arrows are inferred effective immigrants per generation of recipient populations. Significantly positive *g* (population growth parameter) was shown as a plus sign under the name of the mountain ranges (*cox1*/*wg*). Images of *L. formosanus* are redrawn by courtesy of F-L. Yang.

nearly equal migration with YS. Within the Eastern Taiwan, the populations of three mountain ranges had approximately equal migration to each other. A major difference in the gene flow pattern between *cox1* and *wg* is that in *wg* the SS populations contributed more immigrants to WCMR and ALS. Overall, historical gene flows were greater among neighboring populations than distant populations, indicating a pattern of isolation by distance with rare long distance dispersal. Significantly positive values of *g* were detected for populations of ALS, SS, and SCMR (Fig. 5), providing evidence for historical exponential growth in these populations.

3.5. Morphological differentiation and relationships among morphology, genetic divergence, and geographic distance

Statistically significant morphological differentiations were found among five mountain ranges (Table 4). Mandible character A and B together made the greatest contributions to overall morphological differentiation. Pairwise comparisons of morphological variation were significant between most populations located within Western (SS, WCMR, ALS) and Eastern Taiwan (CR, SCMR). Populations of SS with intermediate mandibles displayed the greatest morphological variability in the MDS configuration, and their mandible morphospace overlapped with that of populations from

Table 4
Morphological differentiation between *L. formosanus* populations.

Mountain range	*R* Statistics	*p* value	1st Char. (%)	2nd Char. (%)
ALS vs. SCMR	0.644	0.008	B (34.61)	A (20.34)
ALS vs. CR	0.124	0.048	B (33.33)	A (20.57)
SS vs. CR	0.494	0.009	B (31.44)	A (24.04)
WCMR vs. SCMR	0.516	0.001	B (34.48)	A (20.26)
WCMR vs. CR	0.810	0.007	B (34.74)	A (20.83)

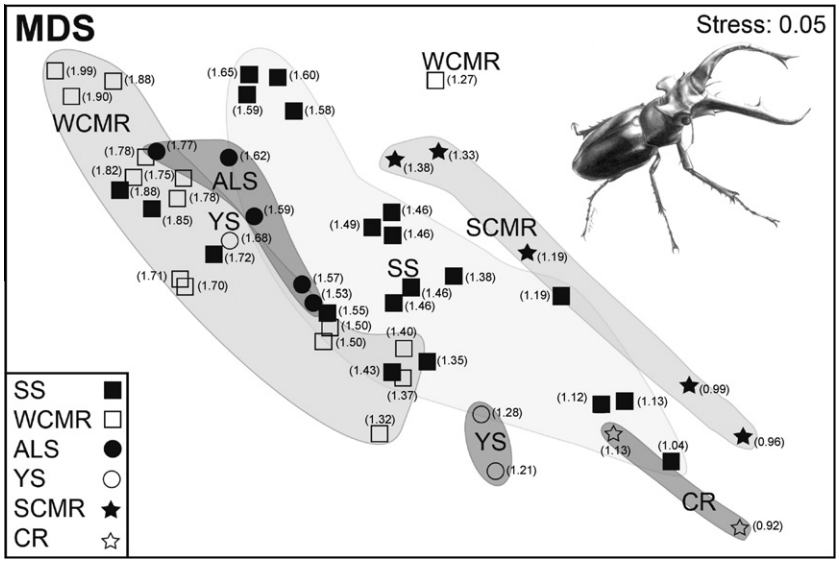

Fig. 6. MDS plot for the morphological measurements of *L. formosanus* populations (global $R = 0.162$, $p = 0.006$). Numbers by the mountain range symbols are standardized average population values of the mandible length divided by the body width [$(A + B)/TW$].

WCMR + ALS with largest mandibles and SCMR + CR with the smallest mandibles (Fig. 6). There was a detectable trend toward decreasing mandible size across populations from Central to Northern Taiwan, and then onto the southeastern part of the island. Mantel tests measuring the level of correlation between morphological differentiations (Euclidean distances) and geographic distances (km) were significant ($r = 0.547$, $p = 0.049$; slope = 0.0017, 95% CI = 0.0001–0.0026) (Fig. 7A). Genetic differentiations (F_{ST}) between populations were also significantly correlated with the geographic distances between populations ($r = 0.484$, $p = 0.013$; slope = 0.0014, 95% CI = 0.0001–0.0020). After controlling the geographic distance as an indicator variable in partial Mantel tests, the pairwise plots of morphological differentiations and genetic distances showed no significant relationship (partial $r = 0.129$, $p = 0.3642$) (Fig. 7B).

4. Discussion

4.1. Discordance between mitochondrial and nuclear data set

This study indicates that the mitochondrial *cox1* and nuclear *wg* gene trees of *L. formosanus* were not fully congruent (Fig. 2). One of the major discrepancies between the two gene trees is that the mitochondrial haplotypes, HYG1 and HYG2 do not cluster with the deeply separated Alishan clade, although in the nuclear data set they appear close to Alishan haplotypes. The mitochondrial haplotype LS3 is located within the Alishan clade, whereas in nuclear reconstructions it does not cluster with the Alishan haplotypes. Despite problems associated with gene tree/species tree incongruence, such results suggest a possible mitochondrial introgression or incomplete sorting of lineages in the ancestral polymorphism of these two markers. In the *cox1* trees, the highly distinct haplotype XD1 has an exceptionally long branch length (Fig. 2A), suggesting that it is either a highly derived haplotype or its phylogenetic position has been incorrectly inferred.

The NCPA of mitochondrial *cox1* and nuclear *wg* genes also resulted in different historical inferences. Allopatric fragmentation and long distance colonization were inferred for *cox1*, whereas the *wg* data set suggested a pattern of restricted gene flow and isolation by distance. Such incongruent inferences can be expected because more profound geographic structures are often observed in mitochondrial genes, which in general show a higher substitution rate and smaller population size than nuclear loci (Avise, 2000; Hare, 2001). Differential dispersal by females and males can also affect the relative degree of phylogeographical structure in mitochondrial and nuclear markers. When males disperse regularly and females are philopatric, maternally inherited markers should have higher levels of population differentiation than biparentally inherited markers. For example, males of the European stag beetles, *L. cervus* have approximately three times the dispersal ability over that of the more philopatric females (Rink and Sinsch, 2007). Therefore, the congeneric *L. formosanus* with a similar life history is also expected to show male-biased dispersal, and therefore higher levels of genetic differentiation among mitochondrial genes than nuclear loci.

4.2. Population history and late Middle Pleistocene expansion

Based on *cox1* gene, this study indicates that *L. formosanus* originated around 1.6 Mya in the Calabrian stage of the early Pleistocene period. The ancestral *L. formosanus* most likely reached Taiwan through emerging land bridges connecting the Asian continent during periodical glaciations when sea levels in the Taiwan Strait were low (Huang et al., 2001). Present *L. formosanus* populations consist of two geographically overlapping haplotype lineages, Alishan and Widespread clades, which are separated by large genetic distances. The deep phylogenetic split between these two largely allopatric lineages may either reflect the accumulation of *de novo* mutations after population separation, or the effects of lineage sorting due to a polymorphic ancestral lineage. Nevertheless, the presence of considerable difference between estimated T_{mrca} of the Alishan and Widespread clades (0.5 vs. 0.7 Mya) and high genetic diversity among these populations imply that extant *L. formosanus* in Taiwan likely originated from two separate refugia. This interpretation is consistent with the findings that Alishan Mountain is geologically younger and confined to a much smaller area than Yushan Mountain and the CMR, where the more ancient Widespread clade originated. Within the Widespread clade, the ancestral haplotypes in the Central lineages subsequently diverged into the more derived haplotypes of the Northern and Southeast lineages.

This study provides the first clear genetic evidence that the Widespread clade of *L. formosanus* experienced a drastic

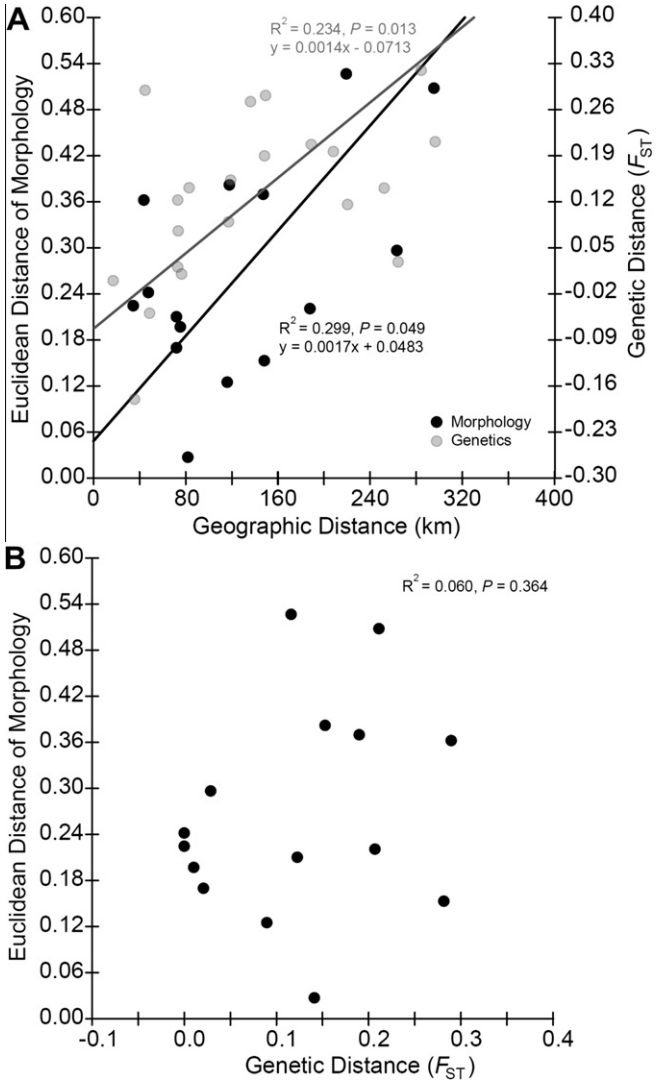

Fig. 7. Pairwise plots of (A) morphological vs. geographic distances and genetic vs. geographic distances, showing for each comparison the slopes of the RMA regression including their equation and correlation coefficient (R^2). (B) Pairwise plots of partial correlation between morphological and genetic distances after controlling for the effect of geographical distances.

population expansion. This expansion started approximately 0.2 million years ago in the late Middle Pleistocene period and lasted for nearly 100,000 years. The onset of this explosive population growth tightly matched the arrival of the Riss glacial period (MIS 6) (Fig. 4), which was the most extensive glacial event from the Middle to Late Pleistocene period (Williams et al., 1998). Climatic oscillations in the Quaternary period dramatically affected the historical demography and geographic distribution of extant taxa (Hewitt, 2000, 2004). This study suggests that the demographic expansion of *L. formosanus* predated the Last Glacial Maximum (LGM) period (about 18,000 years ago) and occupied a much more ancient time frame in the late Middle Pleistocene period in subtropical Taiwan. This historical demographic expansion event likely resulted from altitudinal range shifts of temperate forests in the Middle Pleistocene. During Pleistocene glacial periods in Taiwan, a warm-temperate forest (ca. 500–1800 m) consisting of deciduous *Lauro-Fagetum* species mixed with a few conifers experienced descending altitudinal range shifts and dominated the lowland vegetation (Tsukada, 1966, 1967; Liew and Chung, 2001). Following the vegetation shifts in glacial periods, mid-elevation deciduous forest species like *L. formosanus* descended from higher altitudinal refugia and expanded their distribution in the newly available lowland habitats created by a cooler climate. The continuous temperate forests in the lowlands may also have facilitated *L. formosanus*'s dispersal into previous isolated mid-elevation habitats across different mountain ranges. This historical demographic change in *L. formosanus* population size corroborates the findings that many median- to high-elevation plants in subtropical Taiwan, including the beetle's primary feeding host, *C. glauca*, also experienced a population expansion resulting from altitudinal range shifts into lowlands between Pleistocene glacial cycles (e.g., Huang et al., 2002; Cheng et al., 2005; Chiang et al., 2006).

4.3. Ring-like gene flow and the role of the CMR

This study shows a low overall level of phylogeographic structure as revealed by AMOVA. The genetic structure of *L. formosanus* populations can be characterized by NCPA as restricted gene flow with isolation by distance and rare long distance dispersal among geographically fragmented populations. This pattern of spatially restricted gene flow concurs with the life history characteristics of stag beetles. The life history characteristics of species, including their movement and colonization abilities, determine the dispersal modes and levels of gene flow among populations. Therefore, these characteristics have important genetic and phenotypic consequences (Bohonak, 1999). For *Lucanus* stag beetles, the home range size of females is about 0.2 ha and the migratory movement of females to new nest sites is often less than 1 km, suggesting a limited ability of long distance dispersal to new suitable habitats (Sprecher-Uebersax, 2003; Rink and Sinsch, 2007). Considering this weak dispersal ability and the topographic complexity of CMR, the result of this study reflect a general pattern of short distance, stepping stone dispersal in *L. formosanus*.

A ring-like pattern of gene flow appears among neighboring *L. formosanus* populations near the CMR (Fig. 5). Populations on each side of CMR exhibit substantial historical gene flow, whereas minimal gene exchange occurred between the Eastern and Western populations, which were separated by the CMR. Populations from Eastern and Western Taiwan were genetically connected to each other through exchanging migrants with SS in the northern and SCMR in the southern range of CMR (Figs. 4 and 5). This ring-like pattern of historical gene flow indicates that the CMR, whose peaks above 3000 meters reached their current elevations no later than 1 Mya (Liu et al., 2000; Sibuet and Hsu, 2004; Huang et al., 2006), formed a strong physical barrier to the east–west gene flow of *L. formosanus* distributed at altitudes lower than 1500 m. Although a few Taiwanese taxa exhibit similar genetic structuring generated by the CMR (e.g., Creer et al., 2001; Huang et al., 2002; Cheng et al., 2005; Shih et al., 2006), this study clearly demonstrates a ring-like pattern of gene flow among neighboring populations in the area surrounding CMR.

4.4. Evolution of polyphenic mandibles in L. formosanus

This study finds inconsistent patterns between genetic structures and morphological subdivisions within *L. formosanus* populations. In contrast to low overall phylogeographic structure, we found a geographic cline of decreasing mandible size from Central to North and South, and onto Southeast of Taiwan. After accounting for geographic effect, the evolutionary diversification of the mandible morphology among *L. formosanus* populations does not follow the expected pattern of neutral evolution indicated by the genetic structure of the mitochondrial and nuclear genes. This indicates that mandible variations are most likely subject to sexual or natural selection. Stochastic fluctuations in phenotypic trait values generated purely by mutation and genetic drift are unlikely to produce

a significant correlation between mandible morphology and geography (i.e., environment), nor an apparent geographic cline of mandibular variation. This study provides the first comparative evidence to show that the remarkable within-species variation in mandible morphology of the stag beetle may have an adaptive origin. We hypothesize that the various mandible shapes and sizes in natural *L. formosanus* populations may represent adaptation to habitat heterogeneity.

Like other congeneric *Lucanus* species, *L. formosanus*'s mandibles are developmentally plastic traits that exhibit a linear scaling (allometric) relationship with respect to body size (Huxley, 1931; Kawano, 1997, 2000, 2003; Emlen and Nijhout, 2000; Shinokawa and Iwahashi, 2000; Tatsuta et al., 2001). With changing selective environments, the linear scaling relationships of condition-sensitive traits are capable of rapid divergence through developmental changes, thus evolving steeper or flatter slopes and producing larger or smaller traits (Emlen and Nijhout, 2000; Shingleton et al., 2007). Therefore, the gradient variations of larval diets among mountain ranges may be one of the potential selective agents for the continuous divergence of mandible size. Although there is no direct empirical evidence for the nutritional control of mandible development for any stag beetle species, the observations and laboratory rearing experiments (Kuan & Lin, unpublished data on *Cyclommatus mniszechi*, Lucanidae) suggest that the nutrition of the developing larva likely determines the size and shape of mandibles in *L. formosanus*, along with many secondary sexual traits in other beetles (Emlen, 1994, 1997; Moczek and Emlen, 1999; Emlen and Nijhout, 2000; Karino et al., 2004). Furthermore, the larvae of *L. formosanus* feed on debris of the foliage rather than the decaying woods typically preferred by stag beetles (Lai and Ko, 2008). Thus, the larval food quality derived from continuous variations of forest foliage could be involved in directional natural selection, altering the allometric (scaling) relationships of mandibles in locally adapted *L. formosanus* populations and shifting the mandible morphology of divergent populations into clinal trajectories.

Acknowledgements

We would like to thank C-C. Ko of National Taiwan University, M-M. Yang of National Chung Hsing University, M-L. Chan of National Museum of Natural Science, Y-Y. Yeh of Taiwan Forestry Research Institute, and S-P. Chen of Taiwan Agricultural Research Institute for kindly providing access to their insect collection. We are grateful for the help on insect collecting by Y-W. Huang, J-F. Kuo, Y-S. Liu, L-J. Wang, C-H. Wei, and Tropical Jungle Company. A. Vogler and two anonymous reviewers provided helpful comments on earlier versions of this manuscript. This study was supported by research grants to C-P. Lin from the National Science Council of Taiwan (NSC 94-2621-B-029-004, 94-2311-B-029-007).

Appendix A. Supplementary data

Supplementary data associated with this article can be found, in the online version, at doi:10.1016/j.ympev.2010.10.012.

References

Avise, J.C., 2000. Phylogeography: the history and formation of species. Harvard Univ. Press, Cambridge.
Avise, J.C., 2004. Molecular Markers, Natural History, and Evolution. Sinauer Associates, Sunderland.
Balke, M., Ribera, I., Hendrich, L., Miller, M.A., Sagata, K., Posman, A., Vogler, A., Meier, R., 2009. New Guinea highland origin of a widespread arthropod supertramp. Proc. R. Soc. B 276, 2359–2367.
Beheregaray, L.B., 2008. Twenty years of phylogeography: the state of the field and the challenges for the Southern Hemisphere. Mol. Ecol. 17, 3754–3774.
Bohonak, A., 1999. Dispersal, gene flow, and population structure. Quar. Rev. Biol. 74, 21–45.
Brower, A.V.Z., 1994. Rapid morphological radiation and convergence among races of the butterfly *Heliconicus erato* inferred from patterns of mitochondrial DNA evolution. Proc. Natl. Acad. Sci. USA 91, 6491–6495.
Brower, A.V.Z., DeSalle, R., 1998. Patterns of mitochondrial versus nuclear DNA sequence divergence among nymphalid butterflies: the utility of wingless as a source of characters for phylogenetic inference. Insect Mol. Biol. 7, 1–10.
Brunsfeld, S.J., Sullivan, J., Soltis, D.E., Soltis, P.S., 2001. Comparative phylogeography of northwestern North America: a synthesis. In: Silvertown, J., Antonovics, J. (Eds.), Integrating Ecological and Evolutionary Processes in a Spatial Context. Blackwell, Oxford.
Chang, Y.-J., 2006. Stage Beetles. Yuan-Liou Publisher, Taipei, Taiwan.
Chen, S.-F., Rossiter, S.-J., Faulkes, C.-G., 2006. Population genetic structure and demographic history of the endemic Formosan lesser horseshoe bat (*Rhinolophus monoceros*). Mol. Ecol. 15, 1643–1656.
Cheng, Y.-P., Hwang, S.-Y., Lin, T.-P., 2005. Potential refugia in Taiwan revealed by the phylogeographical study of *Castanopsis carlesii* Hayata (Fagaceae). Mol. Ecol. 14, 2075–2085.
Chiang, Y.-C., Hung, K.-H., Schaal, B.A., Ge, X.-J., Hsu, T.-W., Chiang, T.-Y., 2006. Contrasting phylogeographical patterns between mainland and island taxa of the *Pinus luchuensis* complex. Mol. Ecol. 15, 765–779.
Clarke, K.R., Warwick, R.M., 2001. Change in marine communities: an approach to Statistical Analysis and Interpretation, 2nd edition. PRIMER-E, Plymouth, UK.
Clement, M., Posada, D., Crandall, K., 2000. TCS: a computer program to estimate gene genealogies. Mol. Ecol. 9, 1657–1660.
Creer, S., Malhotra, A., Thorpe, R.S., Chou, W.H., 2001. Multiple causation of phylogeographical pattern as revealed by nested clade analysis of the bamboo viper (*Trimeresurus stejnegeri*) within Taiwan. Mol. Ecol. 10, 1967–1981.
Drummond, A.J., Rambaut, A., 2007. BEAST: Bayesian evolutionary analysis by sampling trees. BMC Evol. Biol. 7, 214–222.
Drummond, A.J., Rambaut, A., Shapiro, B., Pybus, O.G., 2005. Bayesian coalescent inference of past population dynamics from molecular sequences. Mol. Biol. Evol. 22, 1185–1192.
Emlen, D.J., 1994. Environmental control of horn length dimorphism in the beetle *Onthophagus acuminatus* (Coleoptera: Scarabaeidae). Proc. R. Soc. London. Ser. B. 256, 131–136.
Emlen, D.J., 1997. Alternative reproductive tactics and male-dimorphism in the horned beetle *Onthophagus acuminatus* (Coleoptera: Scarabaeidae). Behav. Ecol. Sociobiol. 41, 335–341.
Emlen, D.J., Nijhout, F.H., 2000. The development and evolution of exaggerated morphologies in insects. Annu. Rev. Entomol. 45, 661–708.
Excoffier, L., Laval, G., Schneider, S., 2005. Arlequin (version 3.0): An integrated software package for population genetics data analysis. Evol. Bioinform. 1, 47–50.
Gelman, A., Rubin, D.B., 1992. Inference from iterative simulation using multiple sequences. Stat. Sci. 7, 457–472.
Gibbard, P., van Kolfschoten, T., 2004. The Pleistocene and Holocene Epochs. In: Gradstein, F.M., Ogg, J.G., Smith, G.A. (Eds.), A Geologic Time Scale. Cambridge Univ. Press, Cambridge.
Hare, M.P., 2001. Prospects for nuclear gene phylogeography. Trends Ecol. Evol. 16, 700–706.
Harvey, D.J., Gange, A.C., 2006. Size variation and mating success in the stag beetle, *Lucanus cervus*. Physiol. Entomol. 31, 218–226.
Hewitt, G.M., 1996. Some genetic consequences of ice ages, and their role in divergence and speciation. Biol. J. Linn. Soc. 58, 247–276.
Hewitt, G.M., 2000. The genetic legacy of the Quaternary ice ages. Nature 405, 907–913.
Hewitt, G.M., 2004. Genetic consequences of climatic oscillations in the Quaternary. Philos. Trans. Roy. Soc. B. Biol. Sci. 359, 183–195.
Hsieh, C.F., 2002. Composition, endemism and phytogeographical affinities of the Taiwan flora. Taiwania 47, 298–310.
Huang, C.Y., Xia, K., Yuan, P.B., Chen, P.G., 2001. Structure evolution from Paleogene extension to Latest Miocene-Recent arc-continent collision offshore Taiwan: comparison with on land geology. J. Asian Earth Sci. 19, 619–639.
Huang, S.S.F., Hwang, S.-Y., Lin, T.-P., 2002. Spatial pattern of chloroplast DNA variation of *Cyclobalanopsis glauca* in Taiwan and East Asia. Mol. Ecol. 11, 2249–2358.
Huang, C.Y., Yuan, P.B., Tsao, S.J., 2006. Temporal and spatial records of active arc-continent collision in Taiwan: a synthesis. Bull. Geo. Soc. Am. 118, 274–288.
Hudson, R.R., 2000. A new statistic for detecting genetic differentiation. Genetics 155, 2011–2014.
Huelsenbeck, J.P., Ronquist, F.R., 2001. MrBayes: bayesian inference of phylogeny. Bioinformatics 17, 754–755.
Huxley, J.S., 1931. Relative growth of mandibles in stag beetles (Lucanidae). J. Linn. Soc. Lond. Zool. 37, 675–703.
Hwang, S.Y., Lin, T.P., Ma, C.S., Lin, C.L., Chung, J.D., Yang, J.C., 2003. Postglacial population growth of *Cunninghamia konishii* (Cupressaceae) inferred from phylogeographical and mismatch analysis of chloroplast DNA variation. Mol. Ecol. 12, 2689–2695.
Jensen, J. L., Bohonak, A. J., Kelley, S. T., 2005. Isolation by distance, web service. BMC Genetics. 6: 13. v.3.15 http://ibdws.sdsu.edu/.
Karino, K., Seki, N., Chiba, M., 2004. Larval nutritional environment determines adult size in Japanese horned beetles *Allomyrina dichotoma*. Ecol. Res. 19, 663–668.
Kawano, K., 1997. Cost of evolving exaggerated mandibles in stag beetles (Coleoptera: Lucanidae). Ann. Entomol. Soc. Am. 90, 453–461.
Kawano, K., 2000. Genera and allometry in the stag beetle family Lucanidae. Coleoptera Ann. Entomol. Soc. Am. 93, 198–207.

Kawano, K., 2003. Character displacement in stag beetles (Coleoptera: Lucanidae). Ann. Entomol. Soc. Am. 96, 503–511.
Kodric-Brown, A., Sibly, M., Brown, J.H., 2006. The allometry of ornaments and weapons. Proc. Natl. Acad. Soc. USA 103, 8733–8738.
Kuhner, M.K., 2006. LAMARC 2.0: maximum likelihood and Bayesian estimation of population parameters. Bioinformatics 22, 768–770.
Lai, J., Ko, S.-P., 2008. For the Love of Rhinoceros and Stag Beetles. 2nd Edition. Morning Star Publisher Inc, Taiwan.
Legendre, P., Legendre, L., 1998. Numerical ecology: developments in environmental modeling, no. 20. Elsevier, Amsterdam.
Lessa, E.P., Cook, J.A., Patton, J.L., 2003. Genetic footprints of demographic expansion in North America, but not Amazonia, during the Late Quaternary. Proc. Natl. Acad. Sci. USA 100, 10331–10334.
Liew, P.-M., Chung, N.-J., 2001. Vertical migration of forests during the last glacial period in subtropical Taiwan. W. Pac. Earth. Sci. 1, 405–414.
Lin, R.-C., Yeung, C.K.-L., Li, S.-H., 2008. Drastic post-LGM expansion and lack of historical genetic structure of a subtropical fig-pollinating wasp (*Ceratosolen* sp. 1) of *Ficus* septica in Taiwan. Mol. Ecol. 17, 5008–5022.
Lin, C-P., Huang, J-P., Lee, Y-H., Chen, M-Y., 2009. Phylogenetic position of a threatened stag beetle, *Lucanus datunensis* (Coleoptera: Lucanidae) in Taiwan and implications for conservation. Cons. Genet. Online First, DOI 10.1007/s10592-009-9996-8.
Liu, T.K., Chen, Y.G., Chen, W.S., Jiang, S.H., 2000. Rates of cooling and denudation of the early Penglai Orogeny, Taiwan, as assessed by fission-track constraints. Tectonophysics 320, 69–82.
Maddison, D.R., Maddison, W.P., 2000. MacClade 4: analysis of phylogeny and character, evolution, v. 4.06. Sinauer Associates, Sunderland.
Moczek, A.P., Emlen, D.J., 1999. Proximate determination of male horn dimorphism in the beetle *Onthophagus taurus* (Coleoptera: Scarabaeidae). J. Evol. Biol. 12, 27–37.
Nixon, K.C., 1999. The parsimony ratchet, a new method for rapid parsimony analysis. Cladistics 15, 407–414.
Pons, J., Ribera, I., Bertranpetit, J., Balke, M., 2010. Nucleotide substitution rates for the full set of mitochondrial protein-coding genes in Coleoptera. Mol. Phylogenet. Evol. 56, 796–807.
Posada, D., Crandall, K.A., 1998. MODELTEST: testing the model of DNA substitution. Bioinformatics 14, 817–818.
Posada, D., Crandall, K.A., Templeton, A.R., 2000. GeoDis: a program for the cladistic nested analysis of the geographical distribution of genetic haplotypes. Mol. Ecol. 9, 487–488.
Rambaut, A., Drummond, A. J., 2007. Tracer v1.4, available from http://beast.bio.ed.ac.uk/Tracer.
Ribera, I., Fresneda, J., Bucur, R., Izquierdo, A., Vogler, A.P., Salgado, J.M., Cieslak, A., 2010. Ancient origin of a Western Mediterranean radiation of subterranean beetles. BMC Evol. Biol. 10, 29.
Rink, M., Sinsch, U., 2007. Radio-telemetric monitoring of dispersing stag beetles: implications for conservation. J. Zool. 272, 235–243.
Rogers, A.R., Harpending, H., 1992. Population growth makes waves in the distribution of pairwise genetic differences. Mol. Biol. Evol. 9, 552–569.
Rozas, J., Sánchez-DelBarrio, J.C., Messeguer, X., Rozas, R., 2003. DnaSP, DNA polymorphism analyses by the coalescent and other methods. Bioinformatics 19, 2496–2497.
Shih, H.T., Hung, H.C., Schubart, C.D., Chen, C.A., Chang, H.W., 2006. Intraspecific genetic diversity of the endemic freshwater crab *Candidiopotamon rathbunae* (Decapoda, Brachyura, Potamidae) reflects five million years of the geological history of Taiwan. J. Biogeogr. 33, 980–989.
Shingleton, A.W., Frankino, W.A., Flatt, T., Nijhout, H.F., Emlen, D.J., 2007. Size and shape: the developmental regulation of static allometry in insects. BioEssays 29, 536–548.
Shinokawa, T., Iwahashi, O., 2000. Mating success of small sized males of Japanese stag beetle *Prosopocoilus dissimilis okinawanus* Nomura. Jap. J. Entomol. (N. S.) 3, 157–165.
Sibuet, J.C., Hsu, S.K., 2004. How was Taiwan created? Tectonophysics 379, 159–181.
Sikes, D.S., Lewis, P.O., 2001. PAUPRat: a tool to implement Parsimony Ratchet searches using PAUP. Depart. Ecol. Evol. Biol, Univ. Connecticut, Storrs.
Sprecher-Uebersax, E., 2003. The status of Lucanus cervus in Zwitserland. In: Proceedings of the Second Pan-European Conference on Saproxylic Beetles, pp. 1–3.
Swofford, D.L., 1998. PAUP*: Phylogenetic Analysis Using Parsimony (*and Other Methods), v. 4.0b10. Sinauer Associates, Sunderland.
Tatsuta, H., Mizota, K., Akimoto, S.I., 2001. Allometric patterns of head and genitalia in the stag beetle *Lucanus maculifemoratus* (Coleoptera: Lucanidae). Ann. Entomol. Soc. Am. 94, 462–466.
Tatsuta, H., Mizota, K., Akimoto, S.I., 2004. Relationship between size and shape in the sexually dimorphic beetle *Prosopocoilus inclinatus* (Coleoptera: Lucanidae). Biol. J. Linn. Soc. 81, 219–233.
Templeton, A.R., 2004. Statistical phylogeography: methods of evaluating and minimizing inference errors. Mol. Ecol. 13, 789–809.
Templeton, A.R., 2008. Nested clade analysis: an extensively validated method for strong phylogeographic inference. Mol. Ecol. 17, 1877–1880.
Templeton, A.R., 2009. Statistical hypothesis testing in intraspecific phylogeography: nested clade phylogeographical analysis vs. approximate Bayesian computation. Mol. Ecol. 18, 319–331.
Templeton, A.R., Crandall, K.A., Sing, C.F., 1992. A cladistic analysis of phenotypic associations with haplotypes inferred from restriction endonuclease mapping and DNA sequence data. III. Cladogram estimation. Genetics 132, 619–633.
Templeton, A.R., Routman, E., Phillips, C.A., 1995. Separating population structure from population history: a cladistic analysis of the geographical distribution of mitochondrial DNA haplotypes in the tiger salamander, *Ambystoma tigrinum*. Genetics 140, 767–782.
Tsukada, M., 1966. Late Pleistocene vegetation and climate in Taiwan (Formosa). Proc. Natl. Acad. Sci. USA 55, 543–548.
Tsukada, M., 1967. Vegetation in subtropical Formosa during the Pleistocene glaciation and the Holocene. Palaeogeogr. Palaeoclimatol. Palaeoecol. 3, 49–64.
Wang, H.-Y., 1987. Stag Beetles of Taiwan. Taiwan Museum, Taipei, Taiwan (in chinese).
Wang, H.-Y., 1990. Illustrations of Stag Beetles in Taiwan. Taiwan Museum, Taipei, Taiwan (in Chinese).
Wang, H.-Y., 1994. Guide Book to Insects in Taiwan (5): Lucanidae. Shu-Shin Publisher, Taipei, Taiwan (in Chinese).
Weiss, S., Ferrand, N., 2006. The phylogeography of southern European refugia. Springer, Dordrecht.
Williams, M., Dunkerley, D., De Decker, P., Kershaw, P., Chappell, J., 1998. Quaternary environments. Oxford Univ. Press, New York.
Wüster, W., Ferguson, J.E., Quijada-Mascarenas, J.A., et al., 2005. Tracing an invasion: landbridges, refugia, and the phylogeography of the Neotropical rattlesnake (Serpentes: Viperidae: *Crotalus durissus*). Mol. Ecol. 14, 1095–1108.
Yang, Z., 2007. PAML 4: Phylogenetic analysis by maximum likelihood. Mol. Biol. Evol. 24, 1586–1591.
Yu, H.T., 1994. Distribution and abundance of small mammals along a subtropical elevational gradient in central Taiwan. J. Zool. Lond. 234, 577–600.